VOL.39 Nº3 2022
https://doi.org/10.22259\IMECTA.11271.en

Motion alignment algorithm for a strapdown inertial navigation system

Ana Cristina Vieira Gonçalves*[a],Marcos Ferreira Duarte Pinto*[b],Paulo Cesar Pellanda*[c],
***[a] ana.vieira@ime.eb.br, [b]mpinto11310@gmail.com, [c]pcpellanda@ieee.org**

RESUMO: Este artigo apresenta um novo algoritmo para o alinhamento em movimento de um Sistema de Navegação Inercial do tipo Strapdown (SNIS), com base em um método clássico da literatura. A novidade consiste na introdução de estimativas da repetibilidade dos biases dos sensores inerciais e dos ângulos de atitude de rolagem e arfagem, a partir de observações indiretas e sem auxílio de sensores externos de atitude. O algoritmo permite reiniciar o SNIS sem a necessidade de parar o veículo ou interromper a sua operação durante a navegação, recuperando a precisão do sistema com o veículo em movimento. O alinhamento em movimento evita atrasos de missões ou exposições temporárias do veículo em ambientes perigosos causados por paradas forçadas para alinhamento após a ocorrência de falhas momentâneas, quedas de energia ou desligamentos para manutenção preventiva. O algoritmo é executado em duas etapas, alinhamento grosseiro e fino, ambos usando filtros de Kalman na estimação dos biases dos sensores inerciais e dos erros das variáveis navegacionais do sistema. Com a estimação da repetibilidade dos biases, o SNIS calcula os dados de posição, velocidade e de atitude com maior precisão, a cada período de amostragem. O algoritmo desenvolvido foi validado por meio de simulações da navegação de um navio de guerra.

PALAVRAS-CHAVE: Sistemas inerciais. Alinhamento em movimento. Sensores inerciais.

ABSTRACT: This paper presents a new algorithm for the in-motion alignment of a Strapdown Inertial Navigation System (SNIS), based on a classic method in the literature. The novelty is the introduction of estimates of the repeatability of biases of inertial sensors and roll and pitch attitude angles, based on indirect observations and without the aid of external attitude sensors. The algorithm allows restarting the SNIS without stopping the vehicle or interrupting its operation during navigation, recovering the system's accuracy while it is in motion. In-motion alignment avoids mission delays or temporary exposure of the vehicle in hazardous environments caused by forced stops for alignment after the occurrence of momentary failures, power outages, or shutdowns for preventive maintenance. The algorithm is performed in two steps, coarse and fine alignment, both using Kalman filters to estimate the biases of inertial sensors and the errors of the navigational variables of the system. With the estimation of the repeatability of biases, the SNIS calculates the position, velocity, and attitude data with greater precision at each sampling period. The developed algorithm was validated through simulations of warship navigation.

KEYWORDS: Inertial systems. In-motion alignment. Inertial sensors.

1. Introduction

A Strapdown Inertial Navigation System (SINS) estimates the parameters or navigational variables described by the magnitudes of position, speed and attitude of a vehicle or platform, where it is installed. One of the parameters that make up the position information is the altitude, that is, the local vertical displacement of air or land vehicles. For aquatic and underwater vehicles, in general, altitude refers to heave (vertical linear motion) and depth, respectively. Throughout the text, the term altitude will be used generically to indicate these parameters.

A SINS first performs the alignment process by estimating the initial values of the navigation variables, that is, the initial conditions of the integrators of the differential equations that model the dynamics of the navigation parameters. Then, once the initial conditions are known, the differential equations are integrated into the navigation process and the estimation of the navigational variables is started and carried out continuously. The alignment process can be performed with the SINS stationary or in-motion.

Alignment on the move allows restarting an SINS without the need to stop the vehicle after an interruption in the calculation of navigational variables, whether due to a power outage, malfunction, replacement of sensors or components, or for other reasons. In general, alignment in motion is performed using measurements of navigation parameters provided by external sources installed in the vehicle, such as a supplemental SINS and/or by auxiliary sensors. However, the random errors present in the signals measured by the supplementary SNIS or the auxiliary sensors, added to the errors of the SINS inertial sensors in alignment, they pass to the initial conditions of the dynamic navigation equations and propagated over time, causing increasing drifts in the calculated values of the navigational variables. To reduce initial condition errors, a Kalman Filter (KF) can be introduced into the alignment process.

The FK is a statistical filter developed for application in the context of state space that uses, in its structure, the state transition matrix of the state equations and the sensitivity or observation matrix of the output equations or state measures. In the moving alignment process, the FK states are defined as the difference between the values calculated by the alignment equations and the measurements provided by the auxiliary sensors. This definition implies that the dynamic model of the states is described by differential equations of the errors of the navigation variables of the alignment process, and that the observation equations of the states are a function of the measurements provided by the auxiliary sensors.

Moving alignment is performed in two steps: coarse and fine alignment. For each step of the process, a different structure for the FK is used. The auxiliary sensors used as external sources of position, speed, and altitude for the alignment algorithm are typically the Global Positioning System (GPS), odometer or GPS, and altimeter (or heave sensor/depth gauge), respectively.

The measurements of the inertial sensors and the auxiliary sensors are introduced in the FK structures, in each stage of the alignment, to estimate the errors of the values of the initial conditions (states) of the system and the biases of the inertial sensors.

The alignment processes are performed in closed loop and the new models of the system error dynamics, described in state space, handle large azimuth errors in the coarse alignment and small errors in the fine alignment.

The estimated errors are fed back into the algorithm to correct the navigational parameters calculated by the alignment equations, as well as to compensate for the errors of the inertial sensors in the instrumentation model used in the algorithm.

Consequently, the corrected initial position, attitude and velocity values, at the end of the alignment process, tend towards their real values with specified uncertainties, which are used to initialize the differential equations of the navigation process.

Moving alignment is less discussed in the literature than stationary alignment. Ali; Muhammad [6] presents a moving alignment scheme for a low-cost inertial measurement unit using a consistent and robust FK structure. In the article by Hao et al [7], a non-linear dynamic model for the moving alignment of the inertial navigation system is presented for the case where the observation variables are velocity information. This model is also suitable for transferring navigational parameters from another Inertial Navigation System (INS) present in the vehicle.

Bimal; Joshi [9] presents a non-linear approach to the moving alignment problem using Doppler velocity sensor measurements, considering the initial vehicle attitude information unknown. The wander azimuth frame error models provide partial observability of heading angle error. Alignment simulation is repeated with FK unscented which does not require linearized transform function.

Qi; Pengfei [8] presents a non-linear approach to the moving alignment problem using Doppler velocity sensor measurements, considering the initial vehicle attitude information unknown. The wander azimuth frame error models provide partial observability of heading angle error. Alignment simulation is repeated with FK unscented which does not require linearized transform function.

Alignment in motion has wide application in autonomous and military vehicles. For example, on a warship, the main advantage is to avoid temporary stoppages, which imply mission delays or exposure to dangerous environments.

VOL.39 Nº3 2022
https://doi.org/10.22259\IMECTA.11271.en

The objective of this work is to develop a new moving alignment algorithm, based on a classic method from the literature. [1], to improve the performance and accuracy of estimates of the initial conditions of navigational parameters. In the proposed alignment algorithm, position, velocity and altitude sensors are used. However, assistance is not considered available for measuring the attitude angles, defined by the Euler angles (roll, pitch and heading). Then, the dynamic model of alignment process errors, used in the FK framework, is reformulated to handle large attitude errors, which gradually reduces them until they become small, when another, more adequate model is used to handle small attitude errors.

This article then presents an improvement on the moving alignment algorithm presented by Robert M. Rogers [1]. What is new is the inclusion of the azimuth angular deviation and the repeatability of the biases of the inertial sensors in the state vector of the dynamic model of the SINS errors, increasing its order and the number of variables estimated by the FK. Furthermore, indirect observations of roll and pitch synthesized from accelerometer and altimeter measurements are introduced into the navigation algorithm as if they were auxiliary sensor variables. A blending filter is also used to integrate external altitude sensor (altimeter) measurements. The blending filter increases the calculated altitude bandwidth, attenuates altitude sensor noise, and stabilizes the estimated vertical speed and altitude.

2. Methods

The vectorial physical quantities involved in the alignment and navigation processes of an SNIS can be described based on several references. Depending on the mechanization adopted, it is necessary to express them in the same references chosen for formulating the equations of both processes. [5]

Generally, in an SNIS, the following references are used: Body (b) – $\{X_b,Y_b,Z_b\}$, originates in the CM (Center of Mass) of the body, where is positive longitudinal axis forward, Z_b is positive down and Y_bcompletes the trihedron, according to the right-hand rule; from the Earth (e) –$\{X_e,Y_e,Z_e\}$, has a fixed origin at the Earth's CM, where X_e is the axis of intersection of the Greenwich Meridian with the Equatorial plane, Z_e is parallel and positive with the axis of rotation of the Earth and Y_e complete the trihedron; Inertial (i) – $\{X_i,Y_i,Z_i\}$, originates in the CM of the Earth and fixed in space with its axes initially parallel with the axes of the Earth's reference frame, and the Navigational, which can be the geographic (g) – North-East-Down {N, E, D} ou Wander Azimuth – WA (n) –$\{X_n,Y_n,Z_n\}$ [3].

Figure 1 shows the relationship between the WA (n) and geographic (g) navigational references. The WA frame is rotated with respect to the geographic navigational frame (g) by the wander angle, . The WA frame is important because it avoids attitude singularities that occur when navigating close to the Earth's poles.

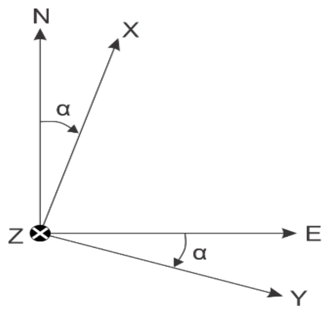

Fig. 1 – Relationship between geographic navigational references (g) - NED and Wander Azimuth-WA (n) – ***Xn-Yn-Zn*** [1].

The Matrix of Director Cosines (MCD) that operates the transformation of the geographic reference (g) to the WA reference (n) is defined as [1],

$$C_g^n = \begin{bmatrix} c\alpha & s\alpha & 0 \\ -s\alpha & c\alpha & 0 \\ 0 & 0 & 1 \end{bmatrix} \quad (1)$$

where s(·) and c(·) represent the trigonometric functions of sine and cosine, respectively.

3. Dynamic navigation equations

The navigation equations will be implemented in the navigational frame WA (n). The equations presented below are also developed in the references [1], [3] and [4].

3.1 Dynamic equations of position

In the mechanization of SNIS in the WA navigational reference frame, the position of a body in the vicinity of the Earth is defined by altitude (h), and by the position angles latitude (L), longitude (l) and *wander angle* (α). These angles are the arguments of the trigonometric functions that form the elements of the position MCD [1],

$$C_e^n = \begin{bmatrix} -c\alpha sLc\ell - s\alpha s\ell & -c\alpha sLc\ell + s\alpha c\ell & c\alpha cL \\ s\alpha sLc\ell - s\alpha c\ell & s\alpha sLs\ell + c\alpha c\ell & -s\alpha cL \\ -cLc\ell & -cLs\ell & -sL \end{bmatrix} \quad (2)$$

which defines the orientation of the Earth frame (e) in relation to the WA navigational frame (n)

The dynamics of the position angles is obtained from the derivative with respect to time of the position matrix C_e^n , defined as:

$$\dot{C}_e^n = -\Omega_{en}^n C_e^n \quad (3)$$

where, Ω_{en}^n the antisymmetric matrix associated with the transport rate vector, ω_{en}^n. The transport speed is the angular speed of the vehicle when it moves over the curved surface of the Earth, and corresponds to the angular speed of the navigational reference frame in relation to the Earth reference frame expressed in the navigational reference frame. The matrix Ω_{en}^n represents the cross product $(\omega_{en}^n \times)$ which in the northern hemisphere is represented as:

$$\omega_{en}^n = \rho = \begin{bmatrix} \rho_x \\ \rho_y \\ \rho_z \end{bmatrix} = \begin{bmatrix} \dfrac{v_y}{(R_y + h)} \\ -\dfrac{v_x}{(R_x + h)} \\ \rho_z \end{bmatrix} \quad (4)$$

where R_y and R_x are the normal and meridional radii of the Earth's curvature, respectively, obtained from the geometric shape of the Earth assumed as an ellipsoid of revolution [10].

In SNIS based on the WA navigational reference, the vertical component of the transport rate is defined as null [3]:

$$\rho_z = 0 \quad (5)$$

Altitude dynamics is defined as the vertical velocity integral, which completes the position states:

$$\dot{h} = v_z^n \quad (6)$$

In this article, for the calculation of altitude, a mixture filter integrated with an external altimeter was introduced to stabilize the calculated altitude.

3.2 Dynamic velocity equations

The dynamic velocity equation developed in the navigational frame (n) is defined as [1]:

$$\dot{v}^n = C_b^n f^b - (2\Omega_{ie}^n + \Omega_{en}^n) \cdot v^n + g^n \quad (7)$$

where, $\dot{v}^n$; the linear velocity vector; f^b is the specific force vector in the body's frame of reference; Ω_{en}^n is the transport rate antisymmetric matrix; Ω_{en}^n is the antisymmetric matrix associated with the Earth's angular velocity vector expressed in the navigational reference frame, g^n ; e ω_{ie}^n is the local normal gravity vector.

3.3 Dynamic attitude equations

The MCD that defines the orientation of the body frame (b) in relation to the WA navigational frame (n) is described as:

$$C_b^n = \begin{bmatrix} c\theta c\psi & -c\phi s\psi + s\phi s\theta c\psi & s\phi s\psi + c\phi s\theta c\psi \\ c\theta s\psi & c\phi c\psi + s\phi s\theta s\psi & -s\phi c\psi + c\phi s\theta s\psi \\ -s\theta & s\phi c\theta & c\phi c\theta \end{bmatrix} \quad (8)$$

where ϕ, θ and ψ are the roll, pitch and heading angles.

The dynamics of the attitude angles is obtained from the derivative with respect to time of the attitude matrix C_b^n defined as [1]:

$$\dot{C}_b^n = C_b^n \Omega_{nb}^n \quad (9)$$

4. Dynamic model of navigation errors

The error model of the navigation parameters is described by the dynamic equations of the position, velocity and attitude errors of the system, expressed in the navigational reference frame WA (n). The model is obtained through linear perturbations of the nominal variables of the dynamic navigation equations (3), (7) and (9). Considering that the perturbations are linear implies assuming that the error terms are small. Thus, the nominal variables plus small errors define the calculated variables that are represented by a superscript bar. The generic expression for the calculated variables is given by:

$$\bar{x} = x + \delta x \quad (10)$$

where, x is the nominal variable, $\bar{x}$ is the calculated value and δx is the small error term.

Substituting the nominal variables of the differential navigation equations for the calculated variables, carrying out the operations with the substituted variables, disregarding error products and subtracting the nominal variables, the dynamic equations of the navigation errors are obtained.

4.1 Dynamic equations of position errors

The calculated position matrix is described as [1]:

$$\bar{C}_e^n = C_e^n + \delta C_e^n \quad (11)$$

where, δC_e^n represents the error of the position matrix (2). The calculated matrix $\bar{C}_e^n$ corresponds to the matrix , tal que, $C_e^n(t+\Delta t)$ such that,

$$C_e^n(t+\Delta t) = [\mathrm{I} - \Delta\Psi] C_e^n(t) \quad (12)$$

The rotation of the nominal matrix C_e^n during the interval Δt is equal to the angle increment produced by the angular position deviations $\delta\theta_x$, $\delta\theta_y$ and $\delta\theta_z$ around the X, Y and Z axes, respectively, which define the position angular deviation vector [1]:

$$\delta\Theta = \left[\delta\theta_x \;\; \delta\theta_y \;\; \delta\theta_z\right]^T \quad (13)$$

The vector $(\delta\Theta_x)$, associated with the antisymmetric matrix $\Delta\Psi$, represents the matrix $\Delta\Psi$ „in (12). Thus, replacing $\Delta\Psi$ by $(\delta\Theta_x)$ in (11) and comparing the equations (11) and (12), we obtain the calculated position matrix:

$$\bar{C}_e^n = C_e^n + \delta C_e^n = [\mathrm{I} - \delta\Theta\times] C_e^n \quad (14)$$

From the equation (14), it turns out that the position matrix error

$$\delta C_e^n = \bar{C}_e^n - C_e^n = -(\delta\Theta\times) C_e^n \quad (15)$$

is a result of angular deviations $\delta\Theta$.

Deriving both members of (15):

$$\delta\dot{C}_e^n = \dot{\bar{C}}_e^n - \dot{C}_e^n = -(\delta\dot{\Theta}\times) C_e^n - (\delta\Theta\times)\dot{C}_e^n \quad (16)$$

Expanding the first member of (16), we obtain:

$$\begin{aligned} \dot{\bar{C}}_e^n - \dot{C}_e^n &= \bar{\Omega}_{en}^n \bar{C}_e^n + \Omega_{en}^n C_e^n \\ &= \bar{\Omega}_{en}^n [\mathrm{I} - (\delta\Theta\times)]_e^n + \Omega_{en}^n C_e^n \\ &\approx -[\bar{\Omega}_{en}^n - \Omega_{en}^n - \Omega_{en}^n (\delta\Theta\times)] C_e^n \end{aligned} \quad (17)$$

and expanding the second member of (17), it arrives at:

$$-(\delta\dot{\Theta}\times) C_e^n - (\delta\Theta\times)\dot{C}_e^n = [(\delta\dot{\Theta}\times) - (\delta\Theta\times)\Omega_{en}^n] C_e^n \quad (18)$$

Comparing both expanded members and rearranging the terms, we obtain the position error matrix dynamic equation,

$$(\delta\Theta\times) = \bar{\Omega}^n_{en} - \Omega^n_{en} - \Omega^n_{en}(\delta\Theta\times) + (\delta\Theta\times)\Omega^n_{en} \quad (19)$$

$$= (\delta\rho\times) - \Omega^n_{en}(\delta\Theta\times) + (\delta\Theta\times)C^n_e$$

and its equivalent in vector form

$$\delta\Theta = \delta\rho - \omega^n_{en} \times \delta\Theta \quad (20)$$

Since the error around the Z axis in the WA reference frame (azimuth error) is solely attributed to the wander angle, it is valid to assume that $\delta\theta_z = 0$, which implies $\delta\dot{\theta}_z = 0$.

Thus, from the third component of $\delta\rho$, in (20), the transport speed error on the Z axis is obtained, as,

$$\delta\rho_z = -\rho_y\delta\theta_x + \rho_x\delta\theta_y \quad (21)$$

The angular position deviations, δΘ, are due to the angular position errors δL, δl and δα. The relationship between them is obtained by substituting the calculated position angles ($\bar{L}$, $\bar{l}$ and $\bar{\alpha}$) in calculated position matrix – first member of equation (14). Comparing with the error expression - second member of (14) –, the following relationships are generated between latitude, longitude and wander angle errors and angular position deviations:

$$\delta L = -s\alpha\,\delta\theta_x - c\alpha\,\delta\theta_y \quad (22.1)$$

$$\delta l = \frac{c\alpha\,\delta\theta_x - s\alpha\,\delta\theta_y}{cL} \quad (22.2)$$

$$\delta\alpha = \delta\theta_z - sL\delta l = -sL\delta l \quad (22.3)$$

4.2 Dynamic equations of speed errors

The dynamic equations of the velocity errors are obtained by replacing the nominal variables in (7) with the calculated variables [1]:

$$\dot{\bar{v}}^n = \bar{f}^n - (\bar{\omega}^n_{en} + 2\bar{\omega}^n_{ie}) \times \bar{v}^n + \bar{g}^n \quad (23)$$

where the calculated quantities follow the general form given in (10):

$$\bar{v}^n = v^n + \delta v^n$$
$$\bar{f}^n = \bar{C}^n_b f^b = (I - (\varphi\times)) f^n + \delta f^n \quad (24)$$
$$\bar{\omega}^n_{en} = \omega^n_{en} + \delta\omega^n_{en}$$
$$\bar{\omega}^n_{ie} = \omega^n_{ie} + \delta\omega^n_{ie}$$
$$\bar{g}^n = g^n + \delta g^n$$

Carrying out the multiplications, ignoring products of errors and subtracting the dynamic equation of the nominal speed, the differential equations of the speed errors are obtained [1]:

$$\delta\dot{v}^n = -(2\delta\omega^n_{ie} + \delta\omega^n_{en}) \times v^n - (2\omega^n_{ie} + \omega^n_{en}) \times \delta v^n + f^n \times \varphi + \delta f^n + \delta g^n \quad (25)$$

where, φ is the vector of angular attitude deviations; $\delta\omega^n_{en}$ and $\delta\omega^n_{ie}$ are the errors of the Earth's transport velocity and angular velocity, defined by [1]:

$$\delta\omega^n_{en} = \left[\left(-\frac{\delta v^n_y}{R_y} - \frac{\delta\rho_x}{R_y}\right)\ \left(-\frac{v^n_x}{R_x} - \frac{\rho_y}{R_x}\delta h\right)\ \delta\rho_z\right]^T \quad (26)$$

and

$$\delta\omega^n_{ie} = \omega^n_{ie} \times \delta\Theta \quad (27)$$

where, $\omega^n_{ie} = [0\ 0\ \Omega]^T$ is the Earth's angular velocity vector, Ω represents the intensity (modulus) of the Earth's angular velocity vector; δf^n is the error vector of the accelerometers; and δg^n is the normal gravity error vector.

4.3 Dynamic equations of attitude errors

The attitude matrix (8) calculated is represented by:

$$\bar{C}^n_b = \left[I - (\varphi^n \times)\right] C^n_b \quad (28)$$

where, φ^n is the vector of the angular deviations of attitude, obtained from the errors of the Euler angles δϕ, δθ and δψ. This vector is represented in the WA frame as:

$$\varphi = [\varphi_x\ \ \varphi_y\ \ \varphi_z\ ]^T \quad (29)$$

Analogously to the position matrix error, the attitude matrix error is obtained by:

$$\delta C_b^n = \bar{C}_b^n - C_b^n = -(\varphi\times)C_b^n \quad (30)$$

Differentiating both sides of the equation (30), generates:

$$\delta \dot{C}_b^n = \dot{\bar{C}}_b^n - \dot{C}_b^n = -(\dot{\varphi}\times)C_b^n - (\varphi\times)\dot{C}_b^n \quad (31)$$

where, the derivative $\dot{C}_b^n$ is given in (9). Replacing the expression (9) in (31) and proceeding with the same operations carried out to calculate the dynamics of position errors, the dynamic equations of attitude errors are obtained:

$$(\dot{\varphi}\times) = -\Omega_{bn}^n(\varphi\times) + (\varphi\times)\Omega_{bn}^n + (\bar{\Omega}_{bn}^n - \Omega_{bn}^n) \quad (32)$$

Or in its equivalent vector form [1]:

$$\dot{\varphi} = \varphi\times\omega_{bn}^n + (\bar{\omega}_{bn}^n - \omega_{bn}^n) \quad (33)$$

The terms in parentheses correspond to the calculated and nominal angular velocities of the body in relation to the navigational frame expressed in the navigational frame. The speeds $\bar{\omega}_{bn}^n$ and ω_{bn}^n are expanded as a function of the angular velocities of the gyroscopes [2]:

$$\omega_{bn}^n = \omega_{in}^n - C_b^n\omega_{ib}^b \text{ e } \bar{\omega}_{bn}^n = \bar{\omega}_{in}^n - \bar{C}_b^n\bar{\omega}_{ib}^b \quad (34)$$

where, the calculated angular velocities of the gyroscopes, expressed in the reference frame of the body in which they are installed, are described by:

$$\bar{\omega}_{ib}^n = \omega_{ib}^n - C_b^n\varepsilon^b \quad (35)$$

The term ε^b represents the vector of random errors of the gyroscopic measurements in the body's reference frame.

Replacing the expressions (34) and (35) in (33) and manipulating the terms of the angular velocities, the most adequate form to represent the dynamic equations of the attitude errors is obtained [1]:

$$(\dot{\varphi}\times) = \delta\omega_{en}^n + \delta\omega_{ie}^n - \omega_{in}^n\times\varphi + C_b^n\varepsilon^b \quad (36)$$

The attitude angular deviation vector, δφ, is produced by the Euler angle errors δϕ, δθ and δψ. The relationship between them is obtained by substituting the calculated Euler angles, $\bar{\phi}$, $\bar{\theta}$ and $\bar{\psi}$, in the calculated attitude matrix – first member of (28) –, and comparing with your error expression – second member of (28) –, the result generates the following expressions for roll, pitch and heading errors as a function of attitude angular deviations:

$$\delta\phi = \frac{s\psi\phi_y - c\psi\phi_x}{c\theta} \quad (37.1)$$

$$\delta\theta = c\psi\phi_y - s\psi\phi_x \quad (37.2)$$

$$\delta\psi = \phi_z(c\psi\phi_x - s\psi\phi_y)\tan\theta \quad (37.3)$$

The alignment in movement assumes that every azimuth error is attributed to the wander angle and, consequently, the angular deviation of attitude in the Z axis is considered null, that is:

$$\varphi_z = 0 \quad (38)$$

5. Alignment in motion

The alignment process can be performed with the system stationary or in motion. Both processes have in common the task of estimating the initial values of the navigational parameters as initial conditions for the integrators of the differential equations of navigation. Once the initial conditions are estimated, the integration operations and the navigation process can be started.

In the stationary alignment process, the SNIS is stopped, so the initial position is known through astronomical references or GPS measurements and the initial velocity is zero. As for the initial attitude, the process performs the self-alignment that uses as references the normal gravity vector, which defines the local vertical, and the horizontal component of the Earth's angular velocity, which points to the North.

Combined with the measurements from the horizontal accelerometers with the vertical reference, the initial pitch and roll angles are approximately determined. The pitch and roll angles define the initial attitude of the SNIS in relation to the local horizontal plane, which determines the angles that level the system. This leveling process is called coarse alignment. Once the initial pitch and roll angles are known, the resulting measurements of the gyroscopes, mounted on the system's horizontal plane, are projected onto the horizontal plane of the navigational reference frame and compared with the horizontal component of Earth's angular velocity to determine the initial heading angle. The initial heading defines the initial alignment of the system itself, in relation to the North direction. At the end of the rough alignment, the initial roll, pitch and heading angles are obtained and the initial attitude of the system is approximately determined.

Inertial sensors are disturbed by deterministic and random errors. Deterministic ones are compensated, and random ones are estimated and then compensated. The random errors of gyroscopes and accelerometers propagate over time in calculating position, velocity and attitude. Thus, it becomes necessary to use a method that estimates the errors of the system's navigational variables. Once the estimated errors are known, they are used to correct the calculated values, refining the leveling and alignment obtained in the coarse alignment phase. This process is known as fine alignment and the estimation is commonly done using an FK.

Both in moving and stationary alignment, the position and initial speeds of the system, in the geographic navigational reference (g), are obtained by the use of auxiliary sensors. The external measurements of position and velocities are also disturbed by random errors and if they were used directly as information of the initial conditions of the differential equations (3) and (7), without the alignment process, they introduced errors in the integration operations of the equations, which would increase over time. The measurements of the position and velocity sensors are used in the observation of the error states of position and velocity of the FK applied in the alignment processes. As for the initial attitude, references to the local gravity vector and the horizontal component of Earth's angular velocity are lost during system motion, and with no auxiliary sensors to measure roll, pitch and heading angles, cannot correctly start the attitude matrix differential equation integration operation (9), due to lack of information on the initial attitude conditions.

To perform the alignment in motion, new hypotheses need to be established to overcome the lack of information on the initial attitude of the system.

In the movement alignment process, wander azimuth mechanization is adopted for the navigational reference. The position aid measures the position variables in the geographic navigational frame (g); thus, the latitude, longitude, and altitude are known, but the wander angle is unknown. Consequently, the position matrix (2) can be partially initialized. Velocity aids measure the initial velocities of the system, so the initial conditions of the differential velocity equations (7) are known and the integration process can be started. With no attitude assist sensors and with the loss of references for the initial attitude calculation, the initial roll, pitch and heading angles are unknown; So, the attitude matrix (8) cannot be initialized.

To solve the position and attitude initialization problem, the following hypotheses are established:

1. it is assumed that the initial attitude angles are all zero; With this hypothesis, the attitude matrix C_b^n is initialized as an identity matrix;
2. it is assumed that the initial wander angle is zero, even though there is the possibility of a large azimuth error, up to 180°; with this assumption the position matrix C_e^n can be initialized;
3. it is assumed that there are no attitude assist sensors;
4. it is assumed that the vehicle maintains a constant linear velocity in the longitudinal direction X_b and zero in the directions Y_b and Z_b, of the body reference (b), as well as the null heading angle, $\psi=0$.

Adopting hypotheses i and ii and using position and velocity sensors, the dynamic equations (3), (7) and (9) are initialized and can be numerically integrated.

VOL.39 Nº3 2022
https://doi.org/10.22259\IMECTA.11271.en

However, as system states will have significant errors, a new system error model is proposed to include large azimuth errors to be used in the FK structure. Based on hypothesis iii, the measures of the attitude angles cannot be obtained, which implies that the observations of the states of the FK attitude errors are not carried out. To work around this problem, hypothesis iv ensures that, using altitude/heave and accelerometer measurements, it is possible to observe the vehicle's roll and pitch angles.

Since the roll and pitch angles are observed, as measured by attitude-aid sensors (magnetometers, for example), the repeatability biases of accelerometers and gyroscopes can be observed indirectly from attitude measurements.

The objective of the moving alignment algorithm, using the new FK structure, is to estimate the position, velocities, repeatability biases of the inertial sensors, attitude and wander angle errors from the possibility of large roll, pitch and wander angle errors, to correct the navigational parameters computed by integrating the dynamic alignment equations. This algorithm that handles large azimuth errors performs a process called coarse alignment.

Based on hypothesis ii, the idea is to associate the large azimuth errors with the errors of the trigonometric functions, sine and cosine of angle , present in the position MCD, and assume that all azimuth error is attributed to the wander angle, which implies that the Z-axis attitude angular deviation is equal to zero, $\phi_z=0$ in (29). This consideration is valid because, in the Wander Azimuth navigational reference frame, the local horizontal plane contains the azimuth angles of the system.

The errors of trigonometric angle functions are defined as:

$$\delta s\alpha = \delta sen\alpha = \overline{sen\alpha} - sen\alpha \quad (39)$$

$$\delta c\alpha = \delta \cos\alpha = \overline{\cos\alpha} - \cos\alpha \quad (40)$$

whose dynamics integrate the state equations of the new system error model to be used in the FK structure for the coarse alignment. [2]

The estimated error states of the trigonometric functions $\delta s\alpha$ and $\delta c\alpha$ are related to the wander angle error by the expression [1]:

$$\delta\alpha = c\alpha\delta\alpha - s\alpha\delta\alpha \quad (41)$$

The estimated wander angle error is used to correct the wander angle calculated using the relation

$$\alpha = \overline{\alpha} - \delta\alpha \quad (42)$$

The new model of the dynamics of navigation errors for large azimuth errors is used in the coarse alignment phase until the error values of the trigonometric functions are reduced to levels considered small. From this limit, a new model for the dynamics of navigation errors is assumed considering small azimuth angle errors. [1] In this model, the wander angle error becomes a direct state to be estimated by the FK, reformulated for small azimuth angle errors. This algorithm that handles small azimuth errors corresponds to the process called fine alignment.

6. Dynamic equations of navigation errors for large azimuth errors

The SNIS errors model for large azimuth angle errors is developed in the wander Azimuth (n) navigational frame and used in the rough alignment.

6.1 Dynamic equations of position errors for large azimuth errors

The dynamic equations of the SNIS position errors subject to large azimuth errors are developed by factoring the nominal position matrix (2) in the following matrix product:

$$C_e^n = C_g^n C_e^g \quad (43)$$

where, C_g^n is given in (1) and C_e^g is defined as [1]:

$$C_e^g = \begin{bmatrix} -sL\,c\ell & -sL\,s\ell & cL \\ -s\ell & c\ell & 0 \\ -cL\,c\ell & -cL\,s\ell & -sL \end{bmatrix} \quad (44)$$

Analogously to (43), the calculated position matrix is factored as:

$$\bar{C}_e^n = \bar{C}_g^n \bar{C}_e^g \quad (45)$$

Expanding the calculated matrix $\bar{C}_g^n$e in terms of the position error matrix between the WA (n) and geographic (g) navigational references, δC_g^n, and the calculated matrix $\bar{C}_e^g$ in terms of the antisymmetric matrix of angular position deviations between the geographic navigational reference frame (g) and the Earth reference frame (e), ($\delta\theta^g\times$), results:

$$\bar{C}_e^n = \left(C_g^n + \delta C_g^n\right)\left[I - \left(\delta\theta^g x\right)\right]C_e^g \quad (46)$$

in terms of the antisymmetric matrix of angular position deviations between the geographic navigational reference frame (g) and the Earth reference frame (e)

$$\delta\theta^g = [\delta\theta_N\ \delta\theta_E\ \delta\theta_D\ ]^T \quad (47)$$

where, $\delta\theta_N$, $\delta\theta_E$ and $\delta\theta_D$ are around the N, E and D axes, respectively.

The calculated matrix $\bar{C}_e^g$ is given by the equation [1]:

$$\bar{C}_e^g = (I - \delta\theta^g x)C_e^g \quad (48)$$

and the error matrix of the trigonometric functions is defined as [1]:

$$\delta C_g^n = \begin{bmatrix} \delta c\alpha & \delta s\alpha & 0 \\ -\delta s\alpha & \delta c\alpha & 0 \\ 0 & 0 & 0 \end{bmatrix} \quad (49)$$

Since every azimuth error, around the Z axis of the system's WA navigational frame, is computed as a wander angle error, it is assumed that, for the rough alignment phase in motion, the angular deviation of position on the vertical axis of the geographic navigational reference frame (g) in relation to the Earth reference frame (e) is null:

$$\delta\theta_D = \delta\theta_Z = 0 \quad (50)$$

which implies

$$\delta\theta_Z = 0 \quad (51)$$

Then, the antisymmetric matrix of the angular deviation of position in the geographic reference is described as:

$$\delta\theta^g = \begin{bmatrix} 0 & 0 & \delta\theta_E \\ 0 & 0 & -\delta\theta_N \\ -\delta\theta_E & \delta\theta_N & 0 \end{bmatrix} \quad (52)$$

Performing the matrix product in (46) and organizing the terms, we obtain:

$$\bar{C}_e^n = \left[I + EC_n^g\right]C_e^n \quad (53)$$

where, the error matrix is given by:

$$E = \begin{bmatrix} \delta c\alpha & \delta s\alpha & -\delta\theta_y \\ -\delta s\alpha & \delta c\alpha & \delta\theta_x \\ \delta\theta_E & -\delta\theta_N & 0 \end{bmatrix} \quad (54)$$

and

$$\delta\theta_x = c\alpha\delta\theta_N + s\alpha\delta\theta_E \quad (55)$$

$$\delta\theta_y = -s\alpha\delta\theta_N + c\alpha\delta\theta_E \quad (56)$$

The matrix E is called the large azimuth error matrix, and its elements correspond to the angular deviations of position, $\delta\theta_x$ and $\delta\theta_y$, plus the errors of the trigonometric functions, $\delta s\alpha$ and $\delta c\alpha$, which correspond to the error model states for large azimuth errors used in the coarse alignment FK.

From the equation (53), we obtain the matrix of position errors as a function of the matrix of large azimuth E errors:

$$\bar{C}_e^n - C_e^n = \delta C_e^n = EC_n^g C_e^n \quad (57)$$

VOL.39 Nº3 2022
https://doi.org/10.22259\IMECTA.11271.en

Deriving the equation (57), we get

$$\delta\dot{C}_e^n = \dot{\tilde{C}}_e^n - \dot{C}_e^n = \dot{E}C_e^g + \dot{C}_e^g E \quad (58)$$

where

$$\dot{C}_e^g = -\Omega_{eg}^g C_e^g \quad (59)$$

and Ω_{eg}^g is the antisymmetric matrix associated with the vector ω_{eg}^g, or ρ^g, which represents the angular velocity of transport of the geographic navigational reference in relation to the Earth reference, defined as:

$$\rho^g = \left[\rho_N \ \ \rho_E \ \ \rho_D\right]^T \quad (60)$$

Substituting the equation (59), considering the condition (6), the expressions of (3) and $\dot{\tilde{C}}_e^n$, the factorizations (43) e (45) and, finally, the error matrix of the trigonometric functions (49), in the equation (58), and then ignoring the products of the errors and rearranging the terms, one can obtain the dynamics of the matrix of large errors of azimuth E, whose elements describe the evolution in time of the angular deviations of position and of the errors of the trigonometric functions:

$$\dot{E} = E\Omega_{eg}^g - \Omega_{en}^n E + \left(\Omega_{en}^n - \bar{\Omega}_{en}^n\right)C_g^n \quad (61)$$

The complete development of the differential equation (61) is presented in Appendix C of the reference [1].

From the derivative of the elements $\delta\theta_x$, $\delta\theta_y$, $\delta s\alpha$ and $\delta c\alpha$ from the matrix $\dot{E}$, the differential equations of the angular deviation of position and the errors of the trigonometric functions are obtained, which integrate the dynamic model of errors used in the FK of the coarse alignment.

During rough alignment, it is assumed that the trigonometric errors are constant. Thus,

$$\delta s\alpha = 0 \quad (62)$$

$$\delta c\alpha = 0 \quad (63)$$

There is a correspondence between the matrix of large azimuth errors, E, and the antisymmetric matrix of angular position deviations ($\delta\Theta\times$), set for small azimuth errors. Comparing the computed position matrices, $\dot{\tilde{C}}_e^n$, given by the equations (14) e (53), results in the relation:

$$-\delta\Theta x \approx EC_n^g \quad (64)$$

The altitude error dynamics is defined as:

$$\delta h = \delta v_z^n \quad (65)$$

6.2 Dynamic equations of velocity errors for large azimuth errors

The dynamics model of velocity errors for large azimuth errors is similar to the model presented in equation (25), with the exception of the earth angular velocity error expressed in the navigational reference frame. This is redefined, based on the relationship given in (64):

$$\delta\omega_{ie}^n = EC_n^g\omega_{ie}^n = E\omega_{ie}^g \quad (66)$$

where $\omega_{ie}^g = \left[\Omega_N \ \ 0 \ \ \Omega_D\right]$is the angular velocity vector of the Earth represented in the geographic navigational frame of reference, and Ω_N and Ω_D are the components in the North and Down directions.

6.3 Dynamic equations of attitude errors for large azimuth errors

The dynamic attitude model for large azimuth errors, in the WA reference frame, is similar to the model presented in equation (36), with the exception of the error of the earth's angular velocity in the navigation frame, as defined in (66). So [1]:

$$\dot{\varphi} = \delta\omega_{en}^n + \delta\omega_{ie}^n - \omega_{in}^n \times \varphi + C_b^n\varepsilon^b \quad (67)$$

where, ω_{in}^n is the angular velocity of the navigational reference in relation to the inertial reference expressed in the navigational reference described in (34).

Expanding the third term of (67), and based on hypothesis ii, which implies (38), a new expression is obtained for the deviation of the transport angular velocity on the axis Z_n:

$$\delta\rho_z = -\Omega_n s\alpha\delta\theta_x - \Omega_n c\alpha\delta\theta_y - \omega_y\delta\phi_x + \omega_x\delta\phi_y - \varepsilon_z \qquad (68)$$

where

$$\omega_x = \omega^g_{iex} + \omega^n_{enx} \qquad (69)$$

$$\omega_y = \omega^g_{iey} + \omega^n_{eny} \qquad (70)$$

7. Dynamic model of coarse alignment errors for large azimuth errors

The coarse alignment process in motion (**figure 2**) employs the dynamic error model that operates on large azimuth errors described by the system of differential equations in state space, defined by the dynamics expressed in (31), (65), (25) e (67), using (66), plus the dynamics of the biases of the inertial sensors described below by the equations (71) e (72). The state variables of the dynamic error model describe the gross alignment errors, represented by the angular position deviations, the altitude error, the velocity errors, the angular deviations of attitude, the errors of the trigonometric functions, and the dynamic models of the biases of the accelerometers and gyroscopes, described as:

$$\delta\dot{B}a = 0 \qquad (71)$$

$$\delta\dot{B}g = 0 \qquad (72)$$

Differently from [1], in this work, the angular deviations of attitude in the Z axis is considered one of the states of the error model, although it was assumed $\phi_z = 0$.

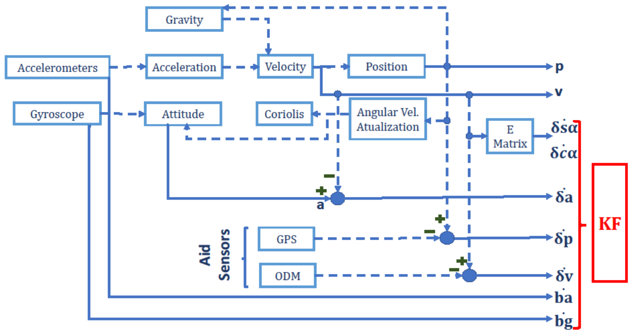

Fig. 2 – Coarse alignment block diagram in motion.

The state vector of the dynamic model of the gross alignment errors is defined as:

$$x_G = \begin{bmatrix} \delta\theta_x & \delta\theta_y & \delta h & \delta v_x & \delta v_y & \delta v_z & \phi_x & \phi_y & \phi_z & \delta s\alpha & \delta c\alpha \\ \delta Ba_x & \delta Ba_y & \delta Ba_z & \delta Bg_x & \delta Bg_y & \delta Bg_z \end{bmatrix}^T \qquad (73)$$

and the dynamic model as:

$$\dot{x}_G = F_G x_G + w_G \qquad (74)$$

where, F_G is the state transition matrix shown in **figure 3** and w_G is the white noise vector of the inertial sensors, defined as:

$$w_G = \begin{bmatrix} 0_{1x3} & \left(-v_y\varepsilon_z + \delta f_x\right) & \left(v_x\varepsilon_z + \delta f_y\right) \\ \delta f_z & \varepsilon_x & \varepsilon_y & \varepsilon_z & 0_{1x8} \end{bmatrix}^T \qquad (75)$$

The state transition matrix of the dynamic error model (**figure 3**) is introduced into the coarse alignment FK structure to estimate the position, velocity, attitude, biases of the inertial sensors and the errors of the trigonometric functions, which implement the correction of the states calculated by the gross alignment equations in the feedback configuration.

8. Model of fine alignment errors for small azimuth errors

Coarse alignment continues to operate until the error variance of the trigonometric functions is reduced.

Then, for the fine alignment process, the dynamic model of large azimuth errors is reformulated to the version of the dynamic error model that operates with small azimuth errors, where the wander angle error, δα, is a state of the dynamic model of fine alignment errors to be estimated directly by the FK.

The estimated wander angle error is related to the error of trigonometric functions by the expressions:

$$\delta s\alpha = c\alpha\delta\alpha \text{ e } \delta c\alpha = -s\alpha\delta\alpha \qquad (76)$$

The dynamics of the wander angle estimated error, δα, is obtained from the expansion of the element (1,1) of the matrix $\dot{E}$, given in (61):

$$\delta\dot{c}\alpha = \delta s\alpha\rho_D + \delta\theta_y\rho_E - \rho_z\delta s\alpha - \rho_y\delta\theta_E - \delta\phi_z s\alpha \qquad (77)$$

$$= \delta s\alpha(\rho_D - \rho_z) + \delta\theta_y\rho_E - \rho_y\delta\theta_E - \delta\phi_z s\alpha$$

$$= -\dot{\alpha}\delta s\alpha + \delta\theta_y\rho_E - \rho_y\delta\theta_E - \delta\phi_z s\alpha$$

where, $\dot{\alpha} = \rho_z - \rho_D$.

Replacing (74) in (76) and transforming the terms ρ_E and $\delta\theta_E$ from the geographic navigational reference to the WA reference, we obtain:

$$\delta\dot{c}\alpha = -\dot{\alpha}\delta s\alpha + s\alpha(\omega_y\delta\theta_x - \omega_x\delta\theta_y - \omega_y\phi_x + \omega_x\phi_y - \varepsilon_z) \qquad (78)$$

Deriving the second equation from (74), we get:

$$\delta\dot{c}\alpha = -\dot{\alpha}\delta s\alpha - s\alpha\,\delta\dot{\alpha} \qquad (79)$$

Comparing (77) with (78), generates the derivative of the wander angle error described by the differential equation:

$$-\delta\alpha = -\omega_y\delta\theta_x + \omega_x\delta\theta_y + \omega_y\phi_x - \omega_x\phi_y + \varepsilon_z \qquad (80)$$

$$\frac{d}{dt}\begin{Bmatrix}\delta\theta_x\\ \delta\theta_y\\ \delta h\\ \delta v_x\\ \delta v_y\\ \delta v_z\\ \phi_x\\ \phi_y\\ \phi_z\\ \delta s\alpha\\ \delta c\alpha\\ \delta B_{ax}\\ \delta B_{ay}\\ \delta B_{az}\\ \delta B_{gx}\\ \delta B_{gy}\\ \delta B_{gz}\end{Bmatrix} = \begin{bmatrix}
0 & 0 & -\frac{v_y}{R^2} & 0 & \frac{1}{R} & 0 & 0 & 0 & 0 & -\rho_y & -\rho_x & 0\,0\,0\,0\,0\,0\\
0 & 0 & \frac{v_x}{R^2} & -\frac{1}{R} & 0 & 0 & 0 & 0 & 0 & \rho_x & -\rho_y & 0\,0\,0\,0\,0\,0\\
0 & 0 & 0 & 0 & 0 & -1 & 0 & 0 & 0 & 0 & 0 & 0\,0\,0\,0\,0\,0\\
-(v_y\Omega_y + 2v_z\Omega_z) & v_y\Omega_x & -\frac{v_x v_z}{R^2} & \frac{v_z}{R} & 2\Omega_z & -(\rho+2\Omega)_y & 0 & -f_z & f_y & 2v_z\omega_x & 0 & 0\,0\,0\,0\,0\,0\\
v_x\Omega_y & -(v_x\Omega_x + 2v_z\Omega_z) & -\frac{v_z v_y}{R^2} & -2\Omega_z & \frac{v_z}{R} & (\rho+2\Omega)_x & f_z & 0 & -f_x & 2v_z\omega_y & 2v_z\omega_x & 0\,0\,0\,0\,0\,0\\
2v_x\Omega_z & 2v_y\Omega_z & \frac{v_x v_x + v_y v_y}{R^2} & 2(\rho+\Omega)_y & -2(\rho+\Omega)_x & 0 & -f_y & f_x & 0 & -2v_x\omega_x & -2v_y\omega_x & 0\,0\,0\,0\,0\,0\\
0 & -\Omega_z & -\omega_y & 0 & \frac{1}{R} & 0 & 0 & \Omega_z & -\omega_y & 0 & \Omega_x & 0\,0\,0\,0\,0\,0\\
\Omega_z & 0 & \frac{v_x}{R^2} & -\frac{1}{R} & 0 & 0 & -\Omega_z & 0 & \omega_x & -\Omega_x & 0 & 0\,0\,0\,0\,0\,0\\
-\omega_y & \omega_x & 0 & 0 & 0 & 0 & \omega_y & -\omega_x & 0 & 0 & 0 & 0\,0\,0\,0\,0\,0\\
0 & 0 & 0 & 0 & 0 & 0 & 0 & 0 & 0 & 0 & 0 & 0\,0\,0\,0\,0\,0\\
0 & 0 & 0 & 0 & 0 & 0 & 0 & 0 & 0 & 0 & 0 & 0\,0\,0\,0\,0\,0\\
0 & 0 & 0 & 0 & 0 & 0 & 0 & 0 & 0 & 0 & 0 & 0\,0\,0\,0\,0\,0\\
0 & 0 & 0 & 0 & 0 & 0 & 0 & 0 & 0 & 0 & 0 & 0\,0\,0\,0\,0\,0\\
0 & 0 & 0 & 0 & 0 & 0 & 0 & 0 & 0 & 0 & 0 & 0\,0\,0\,0\,0\,0\\
0 & 0 & 0 & 0 & 0 & 0 & 0 & 0 & 0 & 0 & 0 & 0\,0\,0\,0\,0\,0\\
0 & 0 & 0 & 0 & 0 & 0 & 0 & 0 & 0 & 0 & 0 & 0\,0\,0\,0\,0\,0\\
0 & 0 & 0 & 0 & 0 & 0 & 0 & 0 & 0 & 0 & 0 & 0\,0\,0\,0\,0\,0
\end{bmatrix}\begin{Bmatrix}\delta\theta_x\\ \delta\theta_y\\ \delta h\\ \delta v_x\\ \delta v_y\\ \delta v_z\\ \phi_x\\ \phi_y\\ \phi_z\\ \delta s\alpha\\ \delta c\alpha\\ \delta B_{ax}\\ \delta B_{ay}\\ \delta B_{az}\\ \delta B_{gx}\\ \delta B_{gy}\\ \delta B_{gz}\end{Bmatrix}$$

Fig. 3 – State transition matrix of the dynamic model of coarse alignment errors.

$$\frac{d}{dt}\begin{Bmatrix}\delta\theta_x\\ \delta\theta_y\\ \delta h\\ \delta v_x\\ \delta v_y\\ \delta v_z\\ \phi_x\\ \phi_y\\ \phi_z\\ -(\delta\alpha)\\ \delta B_{ax}\\ \delta B_{ay}\\ \delta B_{az}\\ \delta B_{gx}\\ \delta B_{gy}\\ \delta B_{gz}\end{Bmatrix} = \begin{bmatrix}
0 & 0 & -\frac{v_y}{R^2} & 0 & \frac{1}{R} & 0 & 0 & 0 & 0 & -\rho_y & 0\,0\,0\,0\,0\,0\\
0 & 0 & \frac{v_x}{R^2} & -\frac{1}{R} & 0 & 0 & 0 & 0 & 0 & -\rho_x & 0\,0\,0\,0\,0\,0\\
0 & 0 & 0 & 0 & 0 & -1 & 0 & 0 & 0 & 0 & 0\,0\,0\,0\,0\,0\\
-(v_y\Omega_y + 2v_z\Omega_z) & v_y\Omega_x & -\frac{v_x v_z}{R^2} & \frac{v_z}{R} & 2\Omega_z & -(\rho+2\Omega)_y & 0 & -f_z & f_y & 2v_z\omega_x & 0\,0\,0\,0\,0\,0\\
v_x\Omega_y & -(v_x\Omega_x + 2v_z\Omega_z) & -\frac{v_z v_y}{R^2} & -2\Omega_z & \frac{v_z}{R} & (\rho+2\Omega)_x & f_z & 0 & -f_x & v_z\omega_y & 0\,0\,0\,0\,0\,0\\
2v_x\Omega_z & 2v_y\Omega_z & \frac{v_x v_x + v_y v_y}{R^2} & 2(\rho+\Omega)_y & -2(\rho+\Omega)_x & 0 & -f_y & f_x & 0 & -2(v_x\omega_x + v_y\omega_y) & 0\,0\,0\,0\,0\,0\\
0 & -\Omega_z & -\frac{v_y}{R^2} & 0 & \frac{1}{R} & 0 & 0 & \Omega_z & -\omega_y & 0 & 0\,0\,0\,0\,0\,0\\
\Omega_z & 0 & \frac{v_x}{R^2} & -\frac{1}{R} & 0 & 0 & -\Omega_z & 0 & \omega_x & 0 & 0\,0\,0\,0\,0\,0\\
-\omega_y & \omega_x & 0 & 0 & 0 & 0 & \omega_y & -\omega_x & 0 & 0 & 0\,0\,0\,0\,0\,0\\
0 & 0 & 0 & 0 & 0 & 0 & 0 & 0 & 0 & 0 & 0\,0\,0\,0\,0\,0\\
0 & 0 & 0 & 0 & 0 & 0 & 0 & 0 & 0 & 0 & 0\,0\,0\,0\,0\,0\\
0 & 0 & 0 & 0 & 0 & 0 & 0 & 0 & 0 & 0 & 0\,0\,0\,0\,0\,0\\
0 & 0 & 0 & 0 & 0 & 0 & 0 & 0 & 0 & 0 & 0\,0\,0\,0\,0\,0\\
0 & 0 & 0 & 0 & 0 & 0 & 0 & 0 & 0 & 0 & 0\,0\,0\,0\,0\,0\\
0 & 0 & 0 & 0 & 0 & 0 & 0 & 0 & 0 & 0 & 0\,0\,0\,0\,0\,0\\
0 & 0 & 0 & 0 & 0 & 0 & 0 & 0 & 0 & 0 & 0\,0\,0\,0\,0\,0
\end{bmatrix}\begin{Bmatrix}\delta\theta_x\\ \delta\theta_y\\ \delta h\\ \delta v_x\\ \delta v_y\\ \delta v_z\\ \phi_x\\ \phi_y\\ \phi_z\\ -(\delta\alpha)\\ \delta B_{ax}\\ \delta B_{ay}\\ \delta B_{az}\\ \delta B_{gx}\\ \delta B_{gy}\\ \delta B_{gz}\end{Bmatrix}$$

Fig. 4 – State transition matrix of the fine alignment error dynamic model.

The state vector of the dynamic model of fine alignment errors is defined as:

$$x_F = [\delta\theta_x \ \delta\theta_y \ \delta h \ \delta v_x \ \delta v_y \ \delta v_z \ \phi_x \ \phi_y \ \phi_z \ -(\delta\alpha) \ \delta Ba_x \ \delta Ba_y \ \delta Ba_z \ \delta Bg_x \ \delta Bg_y \ \delta Bg_z]^T \quad (81)$$

and the dynamic error model is described as:

$$\dot{x}_F = F_F x_F + w_F \quad (82)$$

where F_F is the state transition matrix shown in **figure 4** and w_F is the random error vector of the inertial sensors.

$$w_F = [0_{1x3} \ (-v_y\varepsilon_z + \delta f_x) \ (v_x\varepsilon_z + \delta f_y) \ \delta f_z \ \varepsilon_x \ \varepsilon_y \ \varepsilon_z \ 0_{1x7}]^T \quad (83)$$

9. Measurement equations

The dynamic models of the errors for the coarse and fine alignment are described by the systems of state differential equations given in (74) and (82). To complete the state representation of the alignment steps, it is necessary to describe the equations of observations or measures of the states. The measurement of the errors of the navigational variables are dependent on the measurement of the auxiliary sensors. The auxiliary sensors considered available, both for the coarse alignment and for the fine alignment, are the GPS for position, odometer or GPS for speeds and the altimeter for altitude (heave sensor).

Based on hypotheses iii and iv, the measurements of the speed and altitude aids and the measurements of the accelerometers allow the observation, indirectly, of the roll and pitch angles.

For the pitch angle observation, the vertical velocity calculated by the mix filter [1], expressed in the navigational reference frame, for the coarse and fine alignment v_z^n, is equal to the projection of the longitudinal velocity of the body, v_x^n, in the vertical direction (D) of the navigational frame. The relationship is represented by the expressions [3]:

$$v_x^b = v_z^n sen(\theta) \quad (84)$$

$$\theta = arcsen\left(\frac{v_x^b}{v_z^n}\right) \quad (85)$$

The calculated angle is used as an auxiliary measure for the pitch error, used in the observation of the FK attitude states.

For the observation of the roll angle, hypotheses iii and iv are assumed. From the acceleration equation (7) rewritten in order to explain the values of the specific force in the navigational reference,

$$f^n = \frac{dv}{dt} + (2\Omega_{ie}^n + \Omega_{en}^n)v^n - g^n \quad (86)$$

in which, $\frac{dv}{dt}$, v_y^b and v_z^b are null according to hypothesis iv, and using the measurements of the velocity sensors, the Earth's angular velocity, the gravity and the pitch angle observed in (85), the components of the calculated acceleration f^n, in (86), depend only on roll angles and latitude. Comparing the projections of the acceleration components, expressed in the body's reference frame, $C_n^b f^n$, with accelerometer measurements f_y^b and f_z^b carried out in the body frame, the tangent of the roll angle is observed. The relationship is described by the expressions [3]:

$$sen\phi = \frac{(f_x^n sen\theta + f_z^n coscos\,\theta)f_y^b - f_y^n f_z^b}{(f_x^n sen\theta + f_z^n coscos\,\theta)^2 + f_y^{n\,2}} \quad (87)$$

$$\cos\phi = \frac{(f_x^n sen\theta + f_z^n \cos\theta)f_z^b + f_y^n f_y^b}{(f_x^n sen\theta + f_z^n \cos\theta)^2 + f_y^{n2}} \quad (88)$$

$$\phi = \arctan\left(\frac{sen\phi}{\cos\phi}\right) \quad (89)$$

where, $f_v^n = 2\Omega v_x^b$ (cos cos L senθ-senL cos cos θ) and $f_z^n = \frac{v_x^{b\,2}}{R}(cos \quad \theta)^2 - g$.

From the indirect observations of roll and pitch, it is also possible to indirectly observe the repeatability biases of the accelerometers and gyros, δBa and δBg, respectively. Using the observed roll and pitch angles, their derivatives and the observed velocities obtained by the speed assist sensors, the repeatability biases are calculated from the difference in the measurement of the inertial sensors and the calculated values of the accelerations and angular velocities to which the accelerometers and gyros are submitted.

The observed states for the coarse and fine alignment error models are the same, but the dimensions of the observation matrices differ only by the unobserved states of the wander angle errors. In this way, the measurement equations for both error models are formulated as follows:

$$z = H \cdot x = \begin{bmatrix} I_{3x3} & 0_{3x3} & 0_{3x3} & \Lambda & 0_{3x3} & 0_{3x3} \\ 0_{3x3} & I_{3x3} & 0_{3x3} & \Lambda & 0_{3x3} & 0_{3x3} \\ 0_{3x3} & 0_{3x3} & I_{3x3} & \Lambda & 0_{3x3} & 0_{3x3} \\ 0_{3x3} & 0_{3x3} & 0_{3x3} & \Lambda & I_{3x3} & 0_{3x3} \\ 0_{3x3} & 0_{3x3} & 0_{3x3} & \Lambda & 0_{3x3} & I_{3x3} \end{bmatrix} \begin{bmatrix} \delta\theta_x \\ \delta\theta_y \\ \delta h \\ \delta v_x \\ \vdots \end{bmatrix} + v \quad (90)$$

where H is the state observation matrix (scale factor matrix) for the error models, where $\Lambda=0_{3x2}$ for rough alignment and $\Lambda=0_{3x1}$ for the fine alignment, and v is the noise vector of the position, velocity and indirect attitude sensors [3]:

$$v=[v_{lat} \; v_{long} \; v_h \; v_{vx} \; v_{vy} \; v_{vz} \; v_{roll} \; v_{pitch} \;]^T \quad (91)$$

The v_{roll} and v_{pitch} refer to the accelerometer and velocity sensor noises, as can be seen in the equations (85), (87) e (88).

10. Simulations

In this section, the alignment simulation results, coarse and fine, in motion are presented.

The simulation starts with coarse alignment for 3000 s, followed by fine alignment for another 4200 s, with a total simulation time of 7200 s. In figures 5 to 14, it is possible to observe the occurrence of a discontinuity at instants 3000 s, resulting from the transition from the coarse to the fine alignment algorithm.

The simulations of the alignment algorithms were carried out considering a warship as a vehicle with a predefined trajectory equal to a straight line, in order to facilitate the leveling and keep the wander angle varying at a constant rate. This leads to small values for the attitude angles. In this simulation, the roll and pitch angles were defined by sinusoidal movements, with a maximum amplitude of 2° and a frequency of 0.1 Hz, resulting from a sea state with waves classified as "swell", and the heading angle equal to 0°. The ship moves with a linear velocity of 16 km/h (4.44 m/s) in the longitudinal direction of the body only. For the angular position, the initial conditions were defined as 23º of latitude, 43º of longitude and 35º of wander azimuth, and as for altitude, the minimum value equal to zero.

The random errors of the inertial sensors, biases and white noise were defined as:

a. Accelerometers: repeatability biases $1\times10^{(-3)}$ g (accel. X and Y) and $1\times10^{(-4)}$ g (accel. Z) and standard deviations of $0{,}25\times10^{(-3)}$ g (accel. X and Y) and $0{,}25\times10^{(-4)}$ g (accel. Z); white noise with zero mean and standard deviation of $1\times10^{(-3)}$ g (accel. X e Y) and $1\times10^{(-3)}$ g (accel. Z);

b. Gyros: repeatability bias 0.1 degree/h and standard deviation of 0.025 degree/h; white noise with zero mean and standard deviation of 0.05 degree/h.

The random errors of the position, velocity and altitude sensors were defined as white noise with zero mean and variance, σ, equal to:

a. Position sensor - GPS: standard deviation Lat/Long: σ = 0.0235 degrees (1.5') and altitude: σ = 0.1 m;

b. Speed sensor – odometers/GPS: σ = 0.025 m/s;

c. Heave sensor (5 m max. altitude): σ = 0.0005 m.

It should be noted that the altitude measurement provided by the GPS was used in the observation of the altitude error and the measurement of the heave sensor in the mixture filter.

The errors presented in the following figures are related to the difference between the actual and estimated values.

Figure 5 presents the altitude error during the simulation of the moving alignment, from which the effectiveness, in stabilizing the estimated altitude measurements, of the mixture filter integrated to an altitude sensor can be observed. The altitude error at the end of the simulation is of the order of $10^{(-3)}$ m.

The errors present in the inertial sensors, such as repeatability biases (**figure 6 and 7**) propagate to the navigation equations producing errors in the navigational parameters, which grow with time. Thus, the estimation of these biases significantly improve the results of the inertial system. The estimate of the biases of the X and Y accelerometers is 1 μg, with an error of 0.013 μg and 0.0009 μg, respectively, and for the Z axis, an estimate of 100 μg with an error of 0.001 μg.

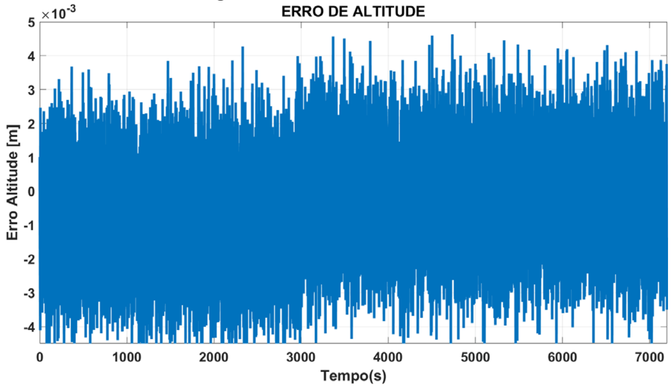

Fig. 5 – Altitude error during the simulation.

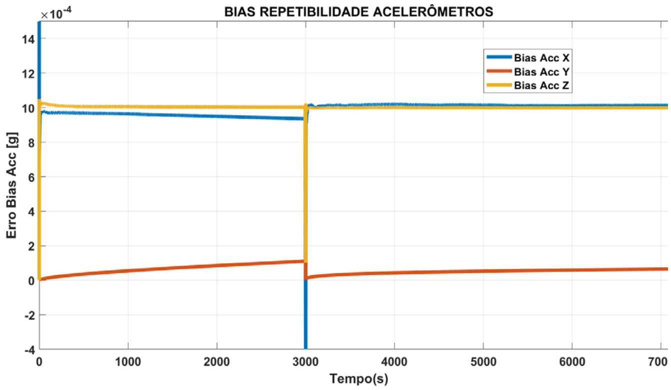

Fig. 6 – Estimation of repeatability of Accelerometer biases: Acc. X (blue), Acc. Y (orange) and Acc. Z (yellow) for all simulation.

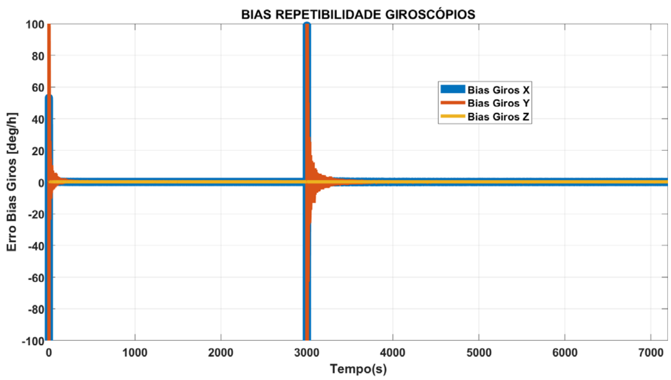

Fig. 7 – Estimation of repeatability of gyroscopes biases: X-gyros (blue), Y-gyros (orange) and Z-gyros (yellow) for the entire simulation.

The estimate of the biases of the X, Y and Z gyroscopes was of the order of 0.1 degree/h with errors of 0.001, 01004 and 0 degree/h for the X, Y and Z, respectively.

In **figure 8**, the latitude and longitude errors are presented. At the initial instant of the alignment, the latitude and longitude values are known, provided by the GPS, consequently the initial error is zero. However, with the passage of time, the errors of angular positions propagate increasing without limit. This behavior is expected in every inertial system due to the impossibility of perfectly estimating the random errors present in inertial sensors, which generate increasing position errors over time.

During the fine alignment, the estimation of the repeatability biases converge to values close to the real ones, which improves the measurement correction of the inertial sensors, reducing the errors of the position angles over time. Correcting the latitude and longitude errors, obtained from equations (22.1) and (22.2) as a function of the estimated position angular deviations, at the end of the simulation, we arrive at an accuracy for latitude of the order of 10^{-5} degrees and for longitude of the order of 10^{-4} degrees.

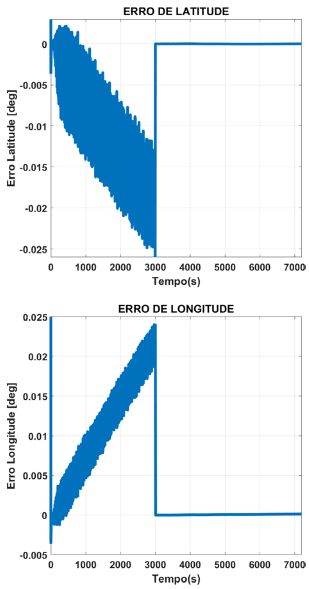

Fig. 8 – Latitude and Longitude error during the simulation.

VOL.39 Nº3 2022
https://doi.org/10.22259\IMECTA.11271.en

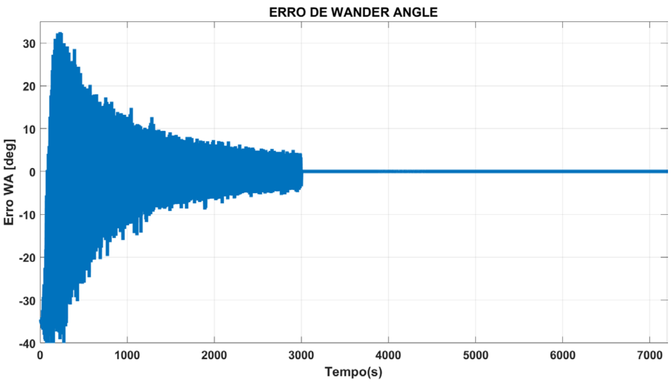

Fig. 9 – Error in the wander angle during the simulation.

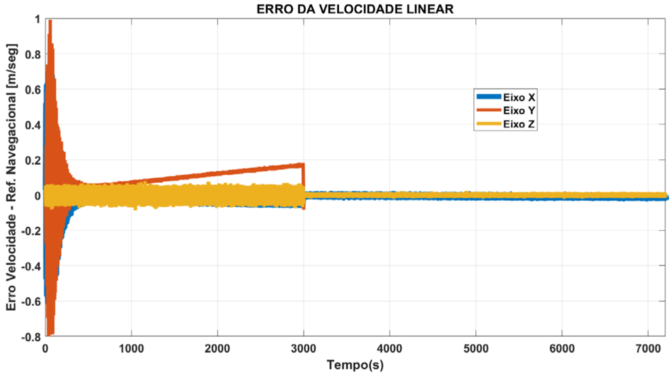

Fig. 10 – Linear velocity error during the simulation.

Figure 9 presents the wander angle error behavior during the moving alignment simulation. To initialize the dynamic position equation (3), the initial wander angle condition for the calculated and estimated values is assumed to be zero. In coarse alignment, the trigonometric errors, δsα and δcα, are states estimated by the FK whose linear combination provides the estimated wander angle error, δα. Correcting the wander angle with δα, it is observed that after 3000 seconds the angle error is approximately 1.5 degrees. Converting to the fine algorithm, where δα is a directly estimated state, the wander angle error at the end of the moving alignment is of the order of 10^{-2} degrees.

Figure 10 shows linear velocity errors in the wander azimuth navigational reference frame during moving alignment. The linear velocity on the Y_n axis would be zero if there were no errors. From Fig. 10, it is observed that at the end of the alignment the error in the direction of the Y_n axis has an accuracy of the order of 10^{-3}. The behavior of the error shows that the use of the mixture filter guarantees the convergence of the linear velocity value on the axis Z_n, v_z^n, for the value corresponding to the vertical projection of the ship's longitudinal linear velocity, of 4.44 m/s aligned with the X_b axis, produced by oscillating the pitch angle. At the end of the alignment, the accuracy of the velocity v_z^n is of the order of 10^{-2}.

The speed on the X_n axis is the horizontal projection of the ship's longitudinal speed (X_b) The graph in **figure 11** shows that the accuracy of the velocity error in the X_n, v_x^n, is 10^{-3} m/s, at the end of the simulation period.

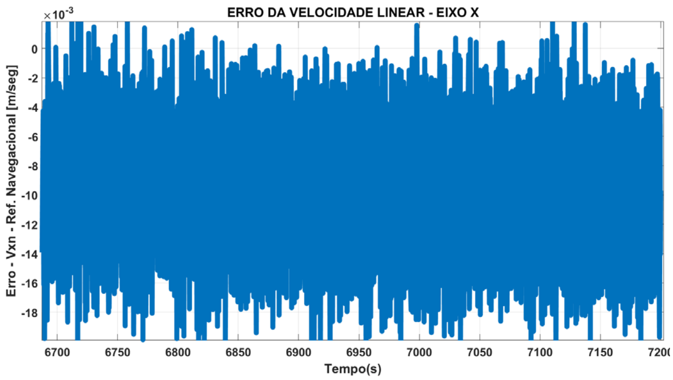

Fig. 11 – Error on the linear velocity X axis at the end of the simulation.

Figures 12, 13 and 14 show the roll, pitch, and heading angle error values for the coarse and fine alignments. The attitude angular deviations, estimated by the FK, are used to calculate the roll and pitch errors according to equations (37), that correct the attitude calculated by the system. In this article, the azimuth angular deviation is included as a state and is estimated. At the end of the alignment, the accuracy of the roll and pitch angles have errors smaller than |0.005| degree, while the heading angle has an accuracy less than |0.02| degree.

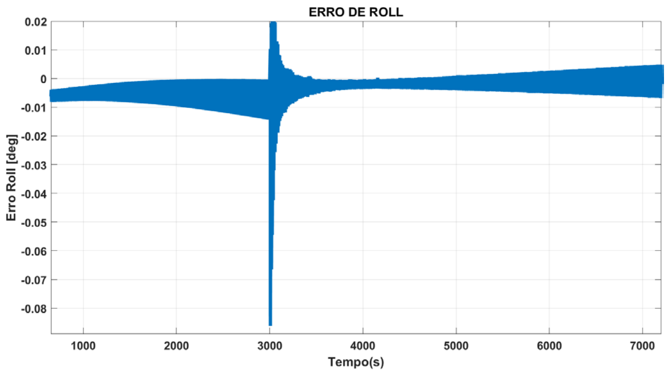

Fig. 12 – Roll angle error during simulation.

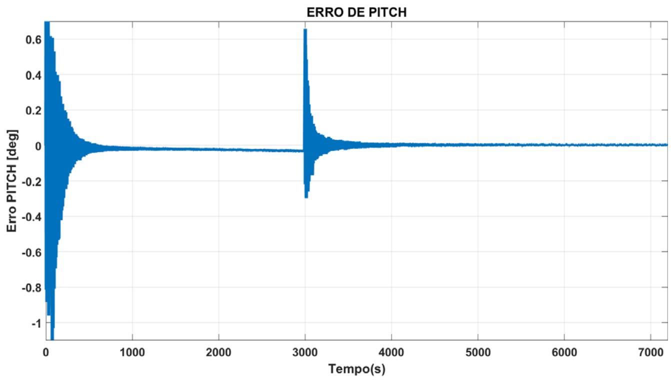

Fig. 13 – Pitch angle error during simulation.

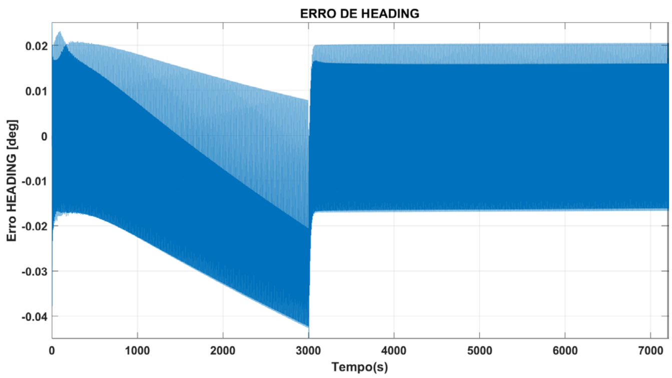

Fig. 14 – Heading angle error during simulation.

11. Conclusions

In this work, the SNIS in-motion alignment algorithm presented by [1] was improved. The improvement consisted of introducing the estimates of the heading angular deviation and the repeatability biases of the inertial sensors in the FK structure. Based on hypotheses iii and iv, a strategy to indirectly observe roll and pitch angles was implemented using accelerometer and altimeter measurements. Furthermore, from these observations, their derivatives of angles and velocity observations, the repeatability biases of inertial sensors could also be observed indirectly. As a consequence, the measures of attitude and biases are estimated, in the simulations carried out, with an accuracy of |0.005|, |0.005| and |0.02| degree for roll, pitch and heading angles, respectively; and errors of 10^{-4} degrees for accelerometers, and 10^{-2} degree for the gyroscopes.

The altimeter measurements are also introduced into an integrated blending filter with the estimated vertical speed, to stabilize the altitude calculated by the system.

The estimation of the repeatability biases implements the compensation of the measurements of the inertial sensors, in the feedback configuration, which provides a significant improvement in the accuracy of the navigation parameters during the SNIS alignment process.

The study points out as a possibility for future work the development of a new model for the error dynamics of a moving alignment algorithm. Such a model would also include the initial estimates of the roll and pitch angles in the initialization and coarse alignment phase of the SNIS and would consider as variables to be estimated, not only the errors of the wander angle trigonometric functions, associated with large azimuth errors, as well as the errors of the trigonometric functions of the attitude, roll and pitch angles.

Acknowledgements

This work was carried out with the support of the Coordination for the Improvement of Higher Education Personnel – Brazil (CAPES) – Financing Code 001.

VOL.39 Nº3 2022
https://doi.org/10.22259\IMECTA.11271.en

References

[1] ROGERS, Robert M. Applied Mathematics in Integrated Navigation Systems. AIAA Education Series. Second Edition. Blacksburg, Virginia. United States of America, 2003.
[2] GONÇALVES, Ana Cristina Vieira. Algoritmo de Alinhamento em Movimento de um Sistema de Navegação Inercial do tipo Strapdown. Instituto Militar de Engenharia. Dissertação de mestrado. Rio de Janeiro. Brasil, 2017.
[3] TITTERTON, D. H.; WESTON, J. L. Strapdown inertial navigation technology. The Institution of Electrical Engineers – IEE. Second Edition. United Kingdom, 2004.
[4] SAVAGE, P.G. Strapdown Inertial Navigation Lectures Notes. Strapdown Associates, Inc. Minnesota. United States of America, 1985.
[5] BRITTING, K. R.. Inertial Navigation Systems Analysis. Cambridge, Massachusetts, April 1971.
[6] ALI, Jamshaid,; MUHAMMAD, Ushaq. A consistent and robust Kalman filter design for in-motion alignment of inertial navigation system. Measurement 42.4 (2009): 577-582.
[7] HAO, Yanling; ZHILAN, Xiong; ZAIGANG Hu. Particle filter for INS in-motion alignment. 1ST IEEE Conference on Industrial Electronics and Applications. IEEE, 2006.
[8] QI, Nie; PENGFEI, Zhao. SINS in-motion alignment for initial attitude uncertainty. In: 2015 Fifth International Conference on Instrumentation and Measurement, Computer, Communication and Control (IMCCC). IEEE, 2015. p. 200-203.
[9] BIMAL, Raj, K.; JOSHI, Ashok. In-motion alignment of inertial navigation system with doppler speed measurements. In: AIAA Guidance, Navigation, and Control Conference. 2015. p. 0096.
[10] World Geodetic System. International Civil Aviation Organization, Second Edition. 1984